

# A backpropagation ANN algorithm based on RGB images for the identification of granite-forming minerals

Alberto Ramil<sup>1</sup>, Ana J. López<sup>2</sup>, Santiago Pozo-Antonio<sup>3</sup>, Teresa Rivas<sup>4</sup>

<sup>1</sup> *Laboratorio de Aplicacións Industriais do Láser, Centro de Investigacións Tecnolóxicas (CIT), Departamento de Enxeñaría Industrial II, Escola Politécnica Superior, Universidade da Coruña, Campus Ferrol, 15403 Ferrol, Spain, alberto.ramil@udc.es*

<sup>2</sup> *Laboratorio de Aplicacións Industriais do Láser, Centro de Investigacións Tecnolóxicas (CIT), Departamento de Enxeñaría Industrial II, Escola Politécnica Superior, Universidade da Coruña, Campus Ferrol, 15403 Ferrol, Spain, ana.xesus.lopez@udc.es*

<sup>3</sup> *Departamento de Enxeñaría dos Recursos Naturais e Medio Ambiente, Escola Superior de Enxeñaría de Minas, Universidade de Vigo, 36310 Vigo, Spain, ipozo@uvigo.es*

<sup>4</sup> *Departamento de Enxeñaría dos Recursos Naturais e Medio Ambiente, Escola Superior de Enxeñaría de Minas, Universidade de Vigo, 36310 Vigo, Spain, trivas@uvigo.es*

**Abstract** – Granite is a rock widely used in the built Cultural Heritage in the NW of Iberian Peninsula. Nowadays, one of the most studied cleaning procedure of the built Cultural Heritage is the laser application because it is gradual and selective. Considering the laser cleaning of granite, it is of great interest to perform the identification of the forming-minerals in the stone surface in order to avoid damage due to the overexposure, improving the treatment results.

The aim of this work is the optimization of a back propagation artificial neural network in order to obtain rapid and reliable identification of forming-minerals in granitic stones by means of RGB images. Our goal is, eventually, *in-situ* monitor the laser cleaning of granite stoneworks. The artificial neural network results obtained were compared with the results of the modal analysis and it was detected a high degree of correct identification of the minerals.

## I. INTRODUCTION

Laser application is a well-established technique used as a cleaning procedure of stones in façades and monuments in the Cultural Heritage (CH) [1, 2]. Different works have been developed using different laser sources, wavelength, stones and surface coatings, mainly in carbonate stones, such as marble and limestones [1, 3]. Among the laser sources investigated; nanosecond- (mainly Nd:YAG or

Nd:YVO<sub>4</sub>), ultrashort- and femtosecond-pulse lasers [4-7].

Granite as the main stone building in the NW of Iberian Peninsula has been investigated in the recent years [8, 9], being these researches centred mainly on the evaluation of the application of different laser sources to clean different types of coatings that affect severely to the CH objects: graffiti, black crust and biological colonization [2 and references therein]. Through all those works, it was observed that the polymineralic composition of this stone with mineral grains with different chemical and physical properties, is the reason of the different behaviours exhibited by each forming mineral after the laser beam action. For instance, biotite melting is a remarkably damage that it was found in the surfaces irradiated with Nd:YVO<sub>4</sub> laser even at low fluence [9]. In addition to biotite fusion, K-feldspar fusion was also detected in an approach to the black crust cleaning with Nd:YAG laser [10]. Also, a pinkish granitic surface experimented some colour changes due to the hue fading of the K-feldspar grains when they were subjected to Nd:YAG laser [11]. Thus, it becomes very important to perform the adjustments of the irradiation parameters to ensure a satisfactory cleaning without any damage of the different forming- mineral of the substrate.

Considering all above, the automatic control of the laser cleaning requires the rapid and reliable identification of the granite forming-minerals in the surface to be irradiated in order to avoid the damages

reported before.

Backpropagation artificial neural network (ANN) algorithms are used widely as solutions to classification and prediction problems in different fields, among them CH studies [12-15].

The main objective of this paper is the identification of granite forming minerals by means of RGB images processed through a backpropagation ANN algorithm in order to attain, eventually, the automatic adjustment of laser irradiation parameters in the laser cleaning avoiding the damage of the granite forming-minerals due to the laser overexposure.

## II. GRANITE SAMPLES

This study was performed over samples of commercial granite from the NW Iberian Peninsula named Rosavel, Rosa Delta and Marrón Estrela. All of them present porphyric texture due to the large size of k-feldspar and plagioclase grains surrounded by an irregular mosaic. Rosavel is pinkish granite with alkali feldspar phenocrysts up to 60 mm length composed of K-feldspar (43 %), quartz (25%), plagioclase (22%), biotite (9%) and accessory minerals (1%). Rosa Delta is a pinkish monzogranite with larger crystals of feldspar and, in a lesser extent plagioclase, reaching up to 5 cm size. It is composed of K-feldspar (45%), quartz (21%), biotite (15%), plagioclase (10%) as main minerals and accessory minerals (9%). Marrón Estrela is a clear-brownish, coarse grained granite, with larger feldspars grains of 2-5 cm size. It is composed of K-feldspar (30 %), quartz (26%), plagioclase (29%), biotite (5%) and accessory minerals (10%) [16].

Samples used in this study were honed slabs of 2 cm thick and 7×15 cm<sup>2</sup> area.

## III. ANN DESIGN AND PERFORMANCE

The ANN used in this work was a conventional feedforward perceptron with a three-layered structure. The weights were optimized through the backpropagation learning algorithm. Owing that the aim of this study was the classification of the major granite forming-minerals; i.e. quartz, feldspars, plagioclase and biotite, four neurons in the output layer were considered with output values between 0 and 1. Regarding the input layer it consisted in three neurons to enter RGB values of each pixel in the image (3 integer values of 8 bits, i. e., between 0 and 255). Furthermore, in this work, different number of hidden neurons was essayed to optimize mineral identification (Fig. 1). The complete process was performed using MatLab Neural Network Toolbox [17].

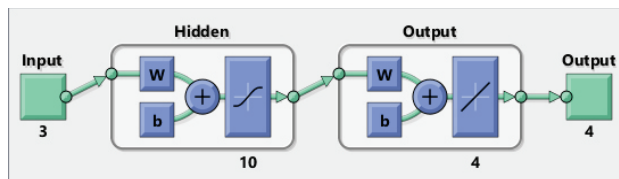


Fig. 1. Schematic diagram of the ANN.

By means of a conventional digital camera, images of the granite slabs were obtained. In these images different regions (sub-images) were selected which correspond to crystal grains of quartz, k-feldspar, plagioclase and biotite. A total of five sub-images were selected for each forming mineral, as it can be appreciated in Fig. 2, which correspond to Rosa Delta granite. Mineral crystals had been previously identified with the help of a microscope.

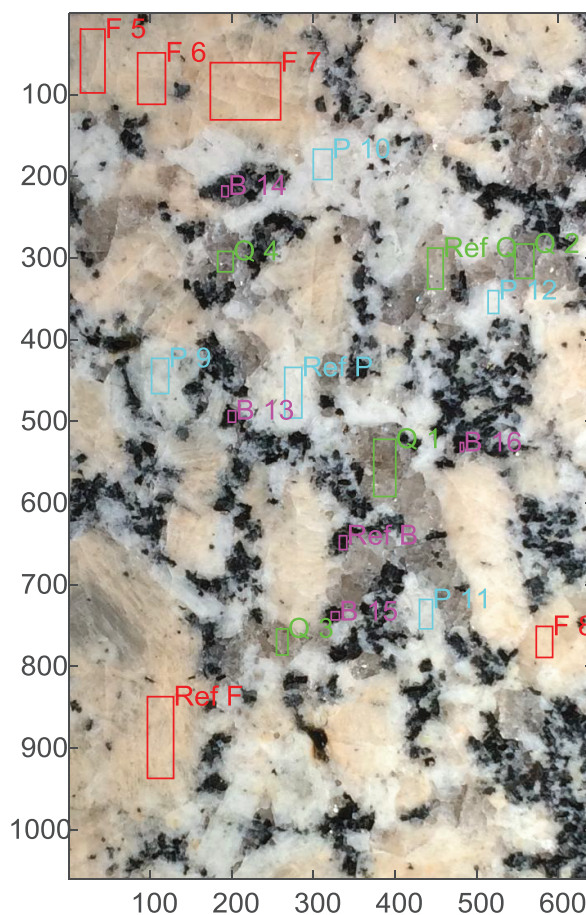


Fig. 2. Image of Rosa Delta granite showing the sub-images which correspond to different mineral crystals. Q: quartz, B: biotite, P: plagioclase, F: K-feldspar

### A ANN training

The number of pixels of each mineral class used for training the network are shown in Table 1 and the histograms of the RGB target data of quartz, K-feldspar, plagioclase and biotite crystals, respectively, can be seen in Fig. 3. The target outputs used in the training process were quartz (1, 0, 0, 0), K-feldspar (0, 1, 0, 0), plagioclase (0, 0, 1, 0) and biotite (0, 0, 0, 1). To evaluate the network performance during training, the 70% of input data was used as training set; 15% as validation set and the remaining 15% was reserved for testing the network. The purpose of validation stage was to determine the stop training to avoid overtraining, i.e., the network loses its ability to generalize. So, the mean square error (MSE) was calculated and the overtraining detected as an increase in MSE of the validation set (see Fig. 4).

Table 1. Number of pixels used to train the networks.

Mineral	Rosavel	Rosa Delta	Marrón Estrela
Quartz	5612	4035	7398
Feldspar	24655	11685	2465
Plagioclase	4081	2915	2838
Biotite	475	457	468

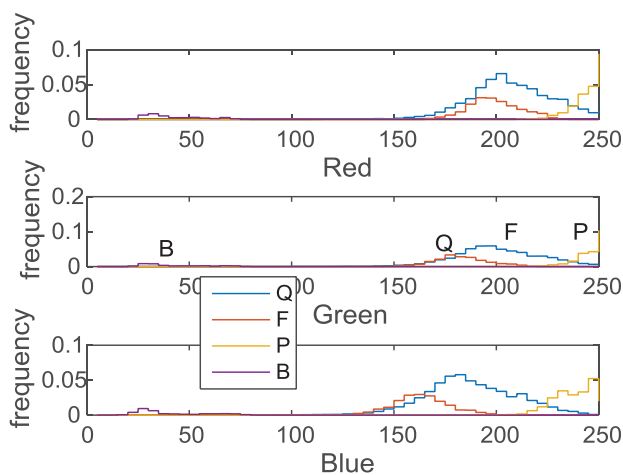


Fig. 3. RGB values of the pixels used to train the network of quartz (Q), K-feldspar (F), plagioclase (P) and biotite (B) minerals.

Furthermore, in this work, test set was used to evaluate the performance of the network as a function of the number of hidden neurons. It can be appreciated (Fig. 5) that depending on the granite, above 5 neurons in hidden layer, a slight improvement in network performance is attained. So the ANN used in this work has 10 neurons in hidden layer.

### B ANN Results

The results obtained; i.e.; ANN output for quartz, K-feldspar, plagioclase and biotite in Rosavel, Rosa Delta and Marrón Estrela granites, are shown in Table 2. As it can be observed, a high percentage of correct assignment was obtained, though some misassignments occur, such as the case of quartz in Rosa Delta, or quartz and K-feldspar in Marron Estrela. Furthermore, minerals allocation in Rosa Delta granite is depicted in Fig.6; the correspondence between mineral crystals in granite slab (Fig. 1) and ANN output can be seen.

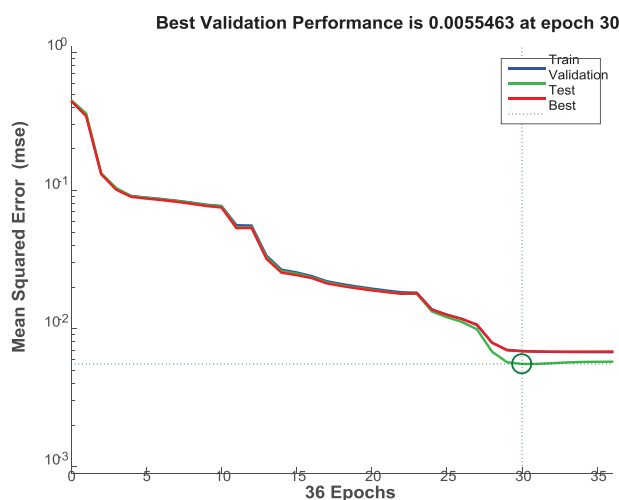


Fig. 4. Mean squared error (MSE) evolution as a function of the number of training epoch. An increase of MSE for the validation dataset indicates overtraining.

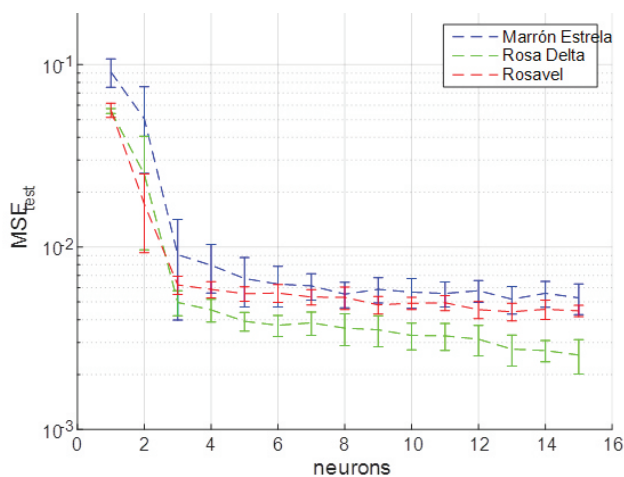


Fig. 5. MSE of test data as a function of neurons in the hidden layer.

On the other side, the ratio (% area) of each mineral in the granite samples, estimated through the neural network results was compared to the modal analysis. The results were in good agreement, especially in the case of Rosavel and Delta Lugo, although, it should be noticed that modal analysis data correspond to % volume, while those obtained through RGB-ANN are % area.

Table 2. Minerals assignation (ANN output) corresponding to the test data input.

Rosavel				
Mineral	% Q	% F	% P	% B
Quartz	96.5	3.4	0.1	0.0
Feldspar	0.2	99.7	0.2	0.0
Plagioclase	0.1	1.3	98.6	0.0
Biotite	0.0	0.0	0.0	100.0
Rosa Delta				
Mineral	% Q	% F	% P	% B
Quartz	47.8	28.0	24.1	0.0
Feldspar	0.0	100.0	0.0	0.0
Plagioclase	2.0	5.2	92.8	0.0
Biotite	0.0	0.0	0.0	100.0
Marrón Estrela				
Mineral	% Q	% F	% P	% B
Quartz	95.8	1.3	3.0	0.0
Feldspar	29.6	70.4	0.1	0.0
Plagioclase	0.0	0.0	100.0	0.0
Biotite	0.0	0.0	0.0	100.0

Table 3. Estimated ratio (% area), obtained from the ANN output, of each of the forming-minerals in the granites.

Mineral	Rosa Delta (% area)	Rosavel (% area)	Marrón Estrela (% area)
Quartz	31.9	24.5	38.5
Feldspar	38.0	46.8	17.5
Plagioclase	18.3	22.3	35.5
Biotite	11.8	6.5	8.6

#### IV. CONCLUSIONS

In this work, they have been presented preliminary results which indicate the suitability of artificial neural networks for identifying crystal minerals of quartz, K-feldspar, plagioclase and biotite in granite by means of RGB data of the digital images. The performance of a

conventional backpropagation three layered perceptron, with three neurons in the input layer and four neurons in the output layer was analysed as a function of the number of epochs of training to improve the ability of minerals identification and avoid overtraining. Furthermore, the number and hidden neurons was also studied. The results of ANN with ten hidden neurons were presented and demonstrated high percentage of correct allocation of the major forming-minerals in Rosavel, Rosa Delta and Marrón Estrela granites.

These results were used to estimate the proportion (% area) of each mineral in the different samples of each granite; getting close to those provided by modal analysis, although with discrepancies which may be due to the latter is calculated as % vol.

Owing that our long-term goal is the automatic identification of granite forming-minerals to develop automatic control of laser cleaning processes, further work is required to improve performance of this method, and its application to mineral identification in other granites.

**Q=green, F=red, P=cyan, B=magenta**

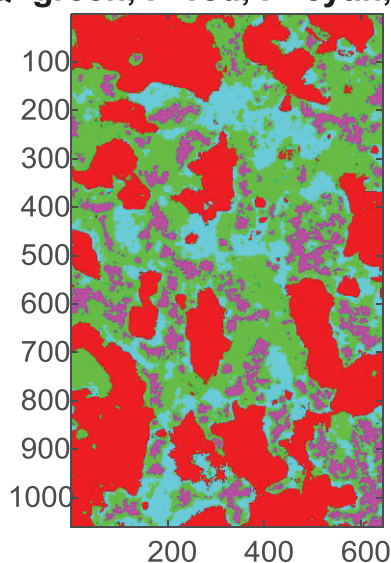


Fig. 6 Estimated allocation of minerals in Rosa Delta granite from ANN output. Q: quartz, F: K-feldspar, P: plagioclase, B: biotite.

#### V. ACKNOWLEDGEMENTS

This work was supported by the Spanish Research Project BIA2014-54186-R. J.S. Pozo-Antonio was supported by a postdoctoral contract with the University of Vigo within the framework of the 2011– 2015 Galicia Plan for Research, Innovation and Growth (Plan I2C) for 2014. The authors would like to thank INGEMARGA S.L., especially to Miguel Martínez.

## REFERENCES

- [1] C. Fotakis, D. Anglos, V. Zafropoulos, S. Georgiou, V. Tornari, "Lasers in the Preservation of Cultural Heritage: Principles and Applications" (Series in Optics and Optoelectronics) 1st edition, Taylor and Francis Group, USA, 2006
- [2] J.S. Pozo-Antonio, T. Rivas, M.P. Fiorucci, A. Ramil, "Effectiveness of granite cleaning procedures in cultural heritage: A review", *Sci. total Environ.*, in press (September 2016)
- [3] P. Pouli, C. Fotakis, B. Hermosin, C. Saiz-Jimenez, C. Domingo, M. Oujja, M. Castillejo, "The laser-induced discoloration of stonework; a comparative study on its origins and remedies", *Spectrochim. Acta A Mol. Biomol. Spectrosc.*, vol.71, N° 3, December 2008, pp. 932- 945
- [4] M. Castillejo, M. Martin, M. Oujja, D. Silva, R. Torres, A. Manousaki, V. Zafropoulos, O.F. van den Brink, R.M.A. Heeren, R. Teule, A. Silva, H. Gouveia, "Analytical study of the chemical and physical changes induced by KrF laser cleaning of tempera paints". *Anal. Chem.*, vol. 74, N° 18, August 2002, pp. 4662–4671.
- [5] A. Moropoulou, S. Kefalonitou, "Efficiency and counter effects of cleaning treatment on limestone surfaces - investigation on the Corfu Venetian Fortress", *Build. Environ.*, vol.37, N° 11, November 2002, pp. 1181–1191.
- [6] M. Oujja, E. Rebollar, M. Castillejo, C. Domingo, C. Cirujano, F. Guerra-Librero, "Laser cleaning of terracotta decorations of the portal of Palos of the Cathedral of Seville", *J. Cult. Herit.*, vol. 6, N° 4, December 2005, pp. 321–327.
- [7] J.R. Vázquez de Aldana, P. Moreno, L. Roso, "Ultrafast lasers: a new frontier for optical materials processing", *Opt. Mater.*, vol. 34, N° 3, January 2012, pp. 572–578.
- [8] T. Rivas, S. Pozo, M.P. Fiorucci, A.J. López, A. Ramil, "Nd:YVO<sub>4</sub> laser removal of graffiti from granite. Influence of paint and rock properties on cleaning efficacy", *Appl. Surf. Sci.*, vol. 263, December 2012, pp. 563-572.
- [9] A.J. López, T. Rivas, J. Lamas, A. Ramil, A. Yáñez, "Optimisation of laser removal of biological crusts in granites", *Appl. Phys. A Mater. Sci. Process.*, vol. 100, N°3, September 2010, pp. 733–739.
- [10] S. Pozo, P Barreiro, T. Rivas, P. González, M.P. Fiorucci, "Effectiveness and harmful effects of removal sulphated black crust from granite using Nd:YAG nanosecond pulsed laser", *Appl. Surf. Sci.* vol. 302, May 2014, pp.309–313
- [11] E. Urones-Garrote, A.J. López, A. Ramil, L.C. Otero-Díaz, " Microstructural study of the origin of color in Rosa Porriño granite and laser cleaning effects", *Appl. Phys. A Mater. Sci. Process.*, vol. 104, N° 1, July 2011, pp. 95–101.
- [12] A. Ramil, A.J. López, A. Yáñez., "Application of artificial neural networks for the rapid classification of archaeological ceramics by means of laser induced breakdown spectroscopy (LIBS)" *Appl. Phys. A*, vol. 92, N° 1, July 2008, pp. 197
- [13] A. López-Molinero, A. Castro, J. Pino, J. Pérez-Arategui, J.R. Castillo, L. Fresenius, "Classification of ancient Roman glazed ceramics using the neural network of Self-Organizing Maps", *Fresenius J. Anal. Chem.*, vol. 367, N° 6, July 2000, pp. 586-595.
- [14] Q.L. Maa, A. Yana, Z. Hu, Z. Lib, B. Fanc, "Principal component analysis and artificial neural networks applied to the classification of Chinese pottery of neolithic age", *Anal. Chim. Acta*, vol. 406, N° 2, February 2000, pp. 247–256
- [15] P. Fermo, F. Cariati, D. Ballabio, V. Consonni, G. Bagnasco Gianni, "Classification of ancient Etruscan ceramics using statistical multivariate analysis of data", *Appl. Phys A*, vol. 79, N° 2, July 2004, pp. 299-307
- [16] UNE-EN 12407:2001. Natural stone test methods. Petrographic examination. AENOR norms (2001)
- [17] H. Demuth, M. Beale, M. Hagan, "Neural Network Toolbox User's Guide" (The MathWorks, Inc. 1992-2007).